

A New Class of Exact Hairy Black Hole Solutions

Theodoros Kolyvaris [†], George Koutsoumbas [‡],
Eleftherios Papantonopoulos ^{*}

Department of Physics, National Technical University of Athens,
Zografou Campus GR 157 73, Athens, Greece

George Siopsis [♭]

Department of Physics and Astronomy, The University of Tennessee,
Knoxville, TN 37996 - 1200, USA

Abstract

We present a new class of black hole solutions with a minimally coupled scalar field in the presence of a negative cosmological constant. We consider an one-parameter family of self-interaction potentials parametrized by a dimensionless parameter g . When $g = 0$, we recover the conformally invariant solution of the Martinez-Troncoso-Zanelli (MTZ) black hole. A non-vanishing g signals the departure from conformal invariance. Thermodynamically, there is a critical temperature at vanishing black hole mass, where a higher-order phase transition occurs, as in the case of the MTZ black hole. Additionally, we obtain a branch of hairy solutions which undergo a first-order phase transition at a second critical temperature which depends on g and it is higher than the MTZ critical temperature. As $g \rightarrow 0$, this second critical temperature diverges.

[†] e-mail address: teokolyv@central.ntua.gr

[‡] e-mail address: kutsugas@central.ntua.gr

^{*} e-mail address: lpapa@central.ntua.gr

[♭] e-mail address: siopsis@tennessee.edu

1 Introduction

Four-dimensional black hole solutions of Einstein gravity coupled to a scalar field have been an avenue of intense research for many years. Questions pertaining to their existence, uniqueness and stability were seeking answers over these years. The Kerr-Newman solutions of four-dimensional asymptotically flat black holes coupled to an electromagnetic field or in vacuum, imposed very stringent conditions on their existence in the form of “no-hair” theorems. In the case of a minimally coupled scalar field in asymptotically flat spacetime the no-hair theorems were proven imposing conditions on the form of the self-interaction potential [1]. These theorems were also generalized to non-minimally coupled scalar fields [2].

For asymptotically flat spacetime, a four-dimensional black hole coupled to a scalar field with a zero self-interaction potential is known [3]. However, the scalar field diverges on the event horizon and, furthermore, the solution is unstable [4], so there is no violation of the “no-hair” theorems. In the case of a positive cosmological constant with a minimally coupled scalar field with a self-interaction potential, black hole solutions were found in [5] and also a numerical solution was presented in [6], but it was unstable. If the scalar field is non-minimally coupled, a solution exists with a quartic self-interaction potential [7], but it was shown to be unstable [8, 9].

In the case of a negative cosmological constant, stable solutions were found numerically for spherical geometries [10, 11] and an exact solution in asymptotically AdS space with hyperbolic geometry was presented in [12] and generalized later to include charge [13]. This solution is perturbatively stable for negative mass and may develop instabilities for positive mass [14]. The thermodynamics of this solution were studied in [12] where it was shown that there is a second order phase transition of the hairy black hole to a pure topological black hole without hair. The analytical and numerical calculation of the quasi-normal modes of scalar, electromagnetic and tensor perturbations of these black holes confirmed this behaviour [15]. Recently, a new exact solution of a charged C-metric conformally coupled to a scalar field was presented in [16, 17]. A Schwarzschild-AdS black hole in five-dimensions coupled to a scalar field was discussed in [18], while Dilatonic black hole solutions with a Gauss-Bonnet term in various dimensions were discussed in [19].

From a known black hole solution coupled to a scalar field other solutions can be generated via conformal mappings [20]. In all black hole solutions in the Einstein frame the scalar field is coupled minimally to gravity. Applying a conformal transformation to these solutions, other solutions can be obtained in the Jordan frame which are not physically equivalent to the untransformed ones [21]. The scalar field in the Jordan frame is coupled to gravity non-minimally and this coupling is characterized by a dimensionless parameter ξ . There are strong theoretical, astrophysical and cosmological arguments (for a review see [21]) which fix the value of this conformal coupling to $\xi = 1/6$. If the scalar potential is zero or quartic in the scalar field, the theory is conformally invariant; otherwise a non-trivial scalar potential introduces a scale in the theory and the conformal invariance is broken.

In this work we present a new class of black hole solutions of four-dimensional Einstein gravity coupled to a scalar field and to vacuum energy. We analyse the structure and

study the properties of these solutions in the Einstein frame. In this frame, the scalar self-interaction potential is characterised by a dimensionless parameter g . If this parameter vanishes, then the known solutions of black holes minimally coupled to a scalar field in (A)dS space are obtained [7, 12]. Transforming these solutions to the Jordan frame, the parameter g can be interpreted as giving the measure of departure from conformal invariance. This breakdown of conformal invariance allows the back-scattering of waves of the scalar field off of the background curvature of spacetime, and the creation of “tails” of radiation. This effect may have sizeable observation signatures in cosmology [22].

Following [23], we perform a perturbative stability analysis of the solutions. We find that the hairy black hole is stable near the conformal point if the mass is negative and may develop instabilities in the case of positive mass. We also study the thermodynamics of our solutions. Calculating the free energy we find that there is a critical temperature above which the hairy black hole loses its hair to a black hole in vacuum. This critical temperature occurs at a point where the black hole mass flips sign, as in the case of the MTZ black hole [12]. Interestingly, another phase transition occurs at a higher critical temperature which is of first order and involves a different branch of our solution. This new critical temperature diverges as the coupling constant in the potential $g \rightarrow 0$. These exact hairy black hole solutions may have interesting applications to holographic superconductors [24, 25], where new types of holographic superconductors can be constructed [14, 26].

Our discussion is organized as follows. In section 2 we introduce the self-interaction potential and we present the hairy black hole solution. In section 3 we discuss the thermodynamics of our solution. In section 4 we perform a stability analysis. Finally, in section 5 we summarize our results.

2 Black Hole with Scalar Hair

To obtain a black hole with scalar hair, we start with the four-dimensional action consisting of the Einstein-Hilbert action with a negative cosmological constant Λ , along with a scalar,

$$I = \int d^4x \sqrt{-g} \left[\frac{R - 2\Lambda}{16\pi G} - \frac{1}{2} g^{\mu\nu} \partial_\mu \phi \partial_\nu \phi - V(\phi) \right], \quad (2.1)$$

where G is Newton’s constant and R is the Ricci scalar. The corresponding field equations are

$$\begin{aligned} G_{\mu\nu} + \Lambda g_{\mu\nu} &= 8\pi G T_{\mu\nu}^{\text{matter}}, \\ \square \phi &= \frac{dV}{d\phi}, \end{aligned} \quad (2.2)$$

where the energy-momentum tensor is given by

$$T_{\mu\nu}^{\text{matter}} = \partial_\mu \phi \partial_\nu \phi - \frac{1}{2} g_{\mu\nu} g^{\alpha\beta} \partial_\alpha \phi \partial_\beta \phi - g_{\mu\nu} V(\phi). \quad (2.3)$$

The potential is chosen as

$$V(\phi) = \frac{\Lambda}{4\pi G} \sinh^2 \sqrt{\frac{4\pi G}{3}} \phi$$

$$+ \frac{g\Lambda}{24\pi G} \left[2\sqrt{3\pi G}\phi \cosh \left(\sqrt{\frac{16\pi G}{3}}\phi \right) - \frac{9}{8} \sinh \left(\sqrt{\frac{16\pi G}{3}}\phi \right) - \frac{1}{8} \sinh \left(4\sqrt{3\pi G}\phi \right) \right] \quad (2.4)$$

and it is given in terms of a coupling constant g . Setting $g = 0$ we recover the action that yields the MTZ black hole [12]. This particular form of the potential is chosen so that the field equations can be solved analytically. The qualitative nature of our results does not depend on the detailed form of the potential. A similar potential was considered in a different context in [5] (see also [26] for the derivation of a potential that yields analytic solutions in the case of a spherical horizon). If one goes over to the Jordan frame, in which the scalar field obeys the Klein-Gordon equation

$$\square\phi - \xi R\phi - \frac{dV}{d\phi} = 0, \quad (2.5)$$

with $\xi = 1/6$, the scalar potential has the form

$$V(\phi) = -\frac{2\pi G\Lambda}{9} \phi^4 - \frac{g\Lambda}{16\pi G} \left[\sqrt{\frac{16\pi G}{3}} \phi \left(1 - \frac{4\pi G}{3} \phi^2 + \frac{\frac{16\pi G}{9} \phi^2}{1 - \frac{4\pi G}{3} \phi^2} \right) - \left(1 - \frac{4\pi G}{3} \phi^2 \right) \left(1 + \frac{4\pi G}{3} \phi^2 \right) \ln \frac{1 + \sqrt{\frac{4\pi G}{3}} \phi}{1 - \sqrt{\frac{4\pi G}{3}} \phi} \right]. \quad (2.6)$$

Evidently, the scalar field is conformally coupled but the conformal invariance is broken by a non-zero value of g .

The mass of the scalar field is given by

$$m^2 = V''(0) = -\frac{2}{l^2} \quad (2.7)$$

where we defined $\Lambda = -3/l^2$. Notice that it is independent of g and coincides with the scalar mass that yields the MTZ black hole [12]. Asymptotically ($r \rightarrow \infty$), the scalar field behaves as $\phi \sim r^{-\Delta_{\pm}}$ where $\Delta_{\pm} = \frac{3}{2} \pm \sqrt{\frac{9}{4} + m^2 l^2}$. In our case $\Delta_+ = 2$ and $\Delta_- = 1$. Both boundary conditions are acceptable as both give normalizable modes. We shall adopt the mixed boundary conditions (as $r \rightarrow \infty$)

$$\phi(r) = \frac{\alpha}{r} + \frac{c\alpha^2}{r^2} + \dots, \quad c = -\sqrt{\frac{4\pi G}{3}} < 0. \quad (2.8)$$

This choice of the parameter c coincides with the MTZ solution [12].

Solutions to the Einstein equations with the boundary conditions (2.8) have been found in the case of spherical horizons and shown to be unstable [23]. In that case, for $\alpha > 0$, it was shown that $c < 0$ always and the hairy black hole had positive mass. On the other hand, MTZ black holes, which have hyperbolic horizons and obey the boundary conditions (2.8) with $c < 0$, can be stable if they have negative mass [14]. This is impossible with

spherical horizons, because they always enclose black holes of positive mass. The numerical value of c is not important (except for the fact that $c \neq 0$) and is chosen as in (2.8) for convenience.

The field equations admit solutions which are black holes with topology $\mathbb{R}^2 \times \Sigma$, where Σ is a two-dimensional manifold of constant negative curvature. Black holes with constant negative curvature are known as topological black holes (TBHs - see, e.g., [27, 28]). The simplest solution for $\Lambda = -3/l^2$ reads

$$ds^2 = -f_{TBH}(\rho)dt^2 + \frac{1}{f_{TBH}(\rho)}d\rho^2 + \rho^2 d\sigma^2 \quad , \quad f_{TBH}(\rho) = \frac{\rho^2}{l^2} - 1 - \frac{\rho_0}{\rho} \quad , \quad (2.9)$$

where ρ_0 is a constant which is proportional to the mass and is bounded from below ($\rho_0 \geq -\frac{2}{3\sqrt{3}}l$), $d\sigma^2$ is the line element of the two-dimensional manifold Σ which is locally isomorphic to the hyperbolic manifold H^2 and of the form

$$\Sigma = H^2/\Gamma \quad , \quad \Gamma \subset O(2, 1) \quad , \quad (2.10)$$

with Γ a freely acting discrete subgroup (i.e., without fixed points) of isometries. The line element $d\sigma^2$ of Σ can be written as

$$d\sigma^2 = d\theta^2 + \sinh^2 \theta d\varphi^2 \quad , \quad (2.11)$$

with $\theta \geq 0$ and $0 \leq \varphi < 2\pi$ being the coordinates of the hyperbolic space H^2 or pseudosphere, which is a non-compact two-dimensional space of constant negative curvature. This space becomes a compact space of constant negative curvature with genus $g \geq 2$ by identifying, according to the connection rules of the discrete subgroup Γ , the opposite edges of a $4g$ -sided polygon whose sides are geodesics and is centered at the origin $\theta = \varphi = 0$ of the pseudosphere. An octagon is the simplest such polygon, yielding a compact surface of genus $g = 2$ under these identifications. Thus, the two-dimensional manifold Σ is a compact Riemann 2-surface of genus $g \geq 2$. The configuration (2.9) is an asymptotically locally AdS spacetime. The horizon structure of (2.9) is determined by the roots of the metric function $f_{TBH}(\rho)$, that is

$$f_{TBH}(\rho) = \frac{\rho^2}{l^2} - 1 - \frac{\rho_0}{\rho} = 0 \quad . \quad (2.12)$$

For $-\frac{2}{3\sqrt{3}}l < \rho_0 < 0$, this equation has two distinct non-degenerate solutions, corresponding to an inner and to an outer horizon ρ_- and ρ_+ respectively. For $\rho_0 \geq 0$, $f_{TBH}(\rho)$ has just one non-degenerate root and so the black hole (2.9) has one horizon ρ_+ . The horizons for both cases of ρ_0 have the non-trivial topology of the manifold Σ . We note that for $\rho_0 = -\frac{2}{3\sqrt{3}}l$, $f_{TBH}(\rho)$ has a degenerate root, but this horizon does not have an interpretation as a black hole horizon.

The boundary has the metric

$$ds_{\mathcal{B}}^2 = -dt^2 + l^2 d\sigma^2 \quad , \quad (2.13)$$

so spatially it is a hyperbolic manifold of radius l (and of curvature $-1/l$).

The action (2.1) with a potential as in (2.4) has a static black hole solution with topology $\mathbb{R}^2 \times \Sigma$ and with scalar hair, and it is given by

$$ds^2 = \frac{r(r+2r_0)}{(r+r_0)^2} \left[-F(r)dt^2 + \frac{dr^2}{F(r)} + r^2 d\sigma^2 \right], \quad (2.14)$$

where

$$F(r) = \frac{r^2}{l^2} - g \frac{r_0}{l^2} r - 1 + g \frac{r_0^2}{l^2} - \left(1 - 2g \frac{r_0^2}{l^2} \right) \frac{r_0}{r} \left(2 + \frac{r_0}{r} \right) + g \frac{r^2}{2l^2} \ln \left(1 + \frac{2r_0}{r} \right), \quad (2.15)$$

and the scalar field is

$$\phi(r) = \sqrt{\frac{3}{4\pi G}} \operatorname{arctanh} \left(\frac{r_0}{r+r_0} \right), \quad (2.16)$$

obeying the boundary conditions (2.8) by design.

3 Thermodynamics

To study the thermodynamics of our black hole solutions we consider the Euclidean continuation ($t \rightarrow i\tau$) of the action in Hamiltonian form

$$I = \int \left[\pi^{ij} \dot{g}_{ij} + p \dot{\phi} - N\mathcal{H} - N^i \mathcal{H}_i \right] d^3x dt + B, \quad (3.1)$$

where π^{ij} and p are the conjugate momenta of the metric and the field respectively; B is a surface term. The solution reads:

$$ds^2 = N^2(r) f^2(r) d\tau^2 + f^{-2}(r) dr^2 + R^2(r) d\sigma^2 \quad (3.2)$$

where

$$N(r) = \frac{r(r+2r_0)}{(r+r_0)^2}, \quad f^2(r) = \frac{(r+r_0)^2}{r(r+2r_0)} F(r), \quad R^2(r) = \frac{r^3(r+2r_0)}{(r+r_0)^2}, \quad (3.3)$$

with a periodic τ whose period is the inverse temperature, $\beta = 1/T$.

The Hamiltonian action becomes

$$I = -\beta \sigma \int_{r_+}^{\infty} N(r) \mathcal{H}(r) dr + B, \quad (3.4)$$

where σ is the area of Σ and

$$\mathcal{H} = NR^2 \left[\frac{1}{8\pi G} \left(\frac{(f^2)'R'}{R} + \frac{2f^2 R''}{R} + \frac{1}{R^2} (1+f^2) + \Lambda \right) + \frac{1}{2} f^2 (\phi')^2 + V(\phi) \right]. \quad (3.5)$$

The Euclidean solution is static and satisfies the equation $\mathcal{H} = 0$. Thus, the value of the action in the classical limit is just the surface term B , which should maximize the action within the class of fields considered.

We now compute the action when the field equations hold. The condition that the geometries which are permitted should not have conical singularities at the horizon imposes

$$T = \frac{F'(r_+)}{4\pi}. \quad (3.6)$$

Using the grand canonical ensemble (fixing the temperature), the variation of the surface term reads

$$\delta B \equiv \delta B_\phi + \delta B_G,$$

where

$$\delta B_G = \frac{\beta\sigma}{8\pi G} \left[N \left(RR' \delta f^2 - (f^2)' R \delta R \right) + 2f^2 R \left(N \delta R' - N' \delta R \right) \right]_{r_+}^\infty, \quad (3.7)$$

and the contribution from the scalar field equals

$$\delta B_\phi = \beta\sigma N R^2 f^2 \phi' \delta \phi|_{r_+}^\infty. \quad (3.8)$$

For the metric, the variation of fields at infinity yields

$$\begin{aligned} \delta f^2|_\infty &= \left(\frac{2}{l^2} r_0 - \frac{2(3 + (9 - 8g)r_0^2/l^2)}{3r} - \frac{4r_0(1 - 4r_0^2/l^2)}{r^2} + \mathcal{O}(r^{-3}) \right) \delta r_0, \\ \delta \phi|_\infty &= \sqrt{\frac{3}{4\pi G}} \left(\frac{1}{r} - \frac{2r_0}{r^2} + \mathcal{O}(r^{-3}) \right) \delta r_0, \\ \delta R|_\infty &= \left(-\frac{r_0}{r} + \frac{3r_0^2}{r^2} + \mathcal{O}(r^{-3}) \right) \delta r_0, \end{aligned} \quad (3.9)$$

so

$$\begin{aligned} \delta B_G|_\infty &= \frac{\beta\sigma}{8\pi G} \left(\frac{6r_0(r - 4(1 - 2g/9)r_0)}{l^2} - 2 + \mathcal{O}(r^{-1}) \right) \delta r_0, \\ \delta B_\phi|_\infty &= \frac{\beta\sigma}{8\pi G} \left(-\frac{6r_0(r - 4r_0)}{l^2} + \mathcal{O}(r^{-1}) \right) \delta r_0. \end{aligned} \quad (3.10)$$

The surface term at infinity is

$$B|_\infty = -\frac{\beta\sigma(3 - 8gr_0^2/l^2)}{12\pi G} r_0. \quad (3.11)$$

The variation of the surface term at the horizon may be found using the relations

$$\begin{aligned} \delta R|_{r_+} &= \delta R(r_+) - R'|_{r_+} \delta r_+, \\ \delta f^2|_{r_+} &= -(f^2)'|_{r_+} \delta r_+. \end{aligned}$$

We observe that $\delta B_\phi|_{r_+}$ vanishes, since $f^2(r_+) = 0$, and

$$\begin{aligned} \delta B|_{r_+} &= -\frac{\beta\sigma}{16\pi G} N(r_+) (f^2)'|_{r_+} \delta R^2(r_+) \\ &= -\frac{\sigma}{4G} \delta R^2(r_+). \end{aligned}$$

Thus the surface term at the horizon is

$$B|_{r_+} = -\frac{\sigma}{4G}R^2(r_+) . \quad (3.12)$$

Therefore, provided the field equations hold, the Euclidean action reads

$$I = -\frac{\beta\sigma(3 - 8gr_0^2/l^2)}{12\pi G}r_0 + \frac{\sigma}{4G}R^2(r_+) . \quad (3.13)$$

The Euclidean action is related to the free energy through $I = -\beta F$. We deduce

$$I = S - \beta M , \quad (3.14)$$

where M and S are the mass and entropy respectively,

$$M = \frac{\sigma(3 - 8gr_0^2/l^2)}{12\pi G} r_0 , \quad S = \frac{\sigma}{4G} R^2(r_+) = \frac{A_H}{4G} \quad (3.15)$$

It is easy to show that the law of thermodynamics $dM = TdS$ holds. For $g = 0$, these expressions reduce to the corresponding quantities for MTZ black holes [12]. Alternatively, the mass of the black hole can be found by the Ashtekar-Das method [29]. A straightforward calculation confirms the expression (3.15) for the mass.

In the case of the topological black hole (2.12) the temperature, entropy and mass are given by respectively,

$$T = \frac{3}{4\pi l} \left(\frac{\rho_+}{l} - \frac{l}{3\rho_+} \right) , \quad S_{TBH} = \frac{\sigma\rho_+^2}{4G} , \quad M_{TBH} = \frac{\sigma\rho_+}{8\pi G} \left(\frac{\rho_+^2}{l^2} - 1 \right) , \quad (3.16)$$

and also the law of thermodynamics $dM = TdS$ is obeyed.

We note that, in the limit $r_0 \rightarrow 0$, $F(r) \rightarrow \frac{r^2}{l^2} - 1$ from eq. (2.15) and the corresponding temperature (3.6) reads $T = \frac{1}{2\pi l}$, which equals the temperature of the topological black hole (3.16) in the limit $\rho_0 \rightarrow 0$ ($\rho_+ \rightarrow 1$). The common limit

$$ds_{\text{AdS}}^2 = - \left[\frac{r^2}{l^2} - 1 \right] dt^2 + \left[\frac{r^2}{l^2} - 1 \right]^{-1} dr^2 + r^2 d\sigma^2 \quad (3.17)$$

is a manifold of negative constant curvature possessing an event horizon at $r = l$. The TBH and our hairy black hole solution match continuously at the critical temperature

$$T_0 = \frac{1}{2\pi l} , \quad (3.18)$$

which corresponds to $M_{TBH} = M = 0$, with (3.17) a transient configuration. Evidently, at the critical point (3.18) a scaling symmetry emerges owing to the fact that the metric becomes pure AdS.

At the critical temperature (3.18) a higher-order phase transition occurs as in the case of the MTZ black hole (with $g = 0$). Introducing the terms with $g \neq 0$ in the potential do not alter this result qualitatively.

Next we perform a detailed analysis of thermodynamics and examine several values of the coupling constant g . Henceforth we shall work with units in which $l = 1$. We begin with a geometrical characteristic of the hairy black hole, the horizon radius r_+ (root of $F(r)$ (eq. (2.15)). In figure 1 we show the r_0 dependence of the horizon for representative values of the coupling constant, $g = 3$ and $g = 0.0005$. We observe that, for $g = 3$, the horizon may correspond to more than one value of the parameter r_0 . For $g = 0.0005$ we see that, additionally, there is a maximum value of the horizon radius.

We note that one may express the radius of the horizon r_+ in terms of the dimensionless parameter

$$\xi = \frac{r_0}{r_+} \quad (3.19)$$

as

$$r_+ = \frac{1 + \xi}{\sqrt{1 + g\xi(1 + \xi)(-1 + 2\xi + 2\xi^2) + \frac{1}{2}g \ln(1 + 2\xi)}}. \quad (3.20)$$

The temperature reads

$$T = \frac{1 + \xi(1 + \xi)(4 - g(1 + 2\xi + 2\xi^2)) + \frac{1}{2}g(1 + 2\xi)^2 \ln(1 + 2\xi)}{2\pi(1 + 2\xi)\sqrt{1 + g\xi(1 + \xi)(-1 + 2\xi + 2\xi^2) + \frac{1}{2}g \ln(1 + 2\xi)}}, \quad (3.21)$$

or equivalently

$$T = \frac{(r_+ + r_0)(r_+^2 + 4r_0r_+ + 4r_0^2 - 8gr_0^3r_+ - 8gr_0^4)}{2\pi r_+^3}, \quad (3.22)$$

a third order equation in r_+ , showing that, for a given temperature, there are in general three possible values of ξ . Thus we obtain up to three different branches of our hairy black hole solution.

We start our analysis with a relatively large value of the coupling constant g , namely $g = 3$ and calculate the horizon radius, temperature and Euclidean action for various values of r_0 . In figure 2, left panel, we depict r_0 versus T and it is clear that there is a T interval for which there are really three corresponding values for r_0 . Outside this interval, there is just one solution. The corresponding graph for the Euclidean actions may be seen in the right panel of the same figure. The action for the topological black hole with the common temperature T is represented by a continuous line, while the actions for the hairy black holes are shown in the form of points. We note that equation (2.12) yields for the temperature of the topological black hole $T = \frac{1}{4\pi} \left(\frac{3\rho_+}{l^2} + \frac{1}{\rho_+} \right) \Rightarrow \rho_+ = \frac{2\pi T}{3} + \sqrt{\left(\frac{2\pi T}{3} \right)^2 - \frac{1}{3}}$. The largest Euclidean action (smallest free energy) will dominate.

There are three branches for the hairy black hole, corresponding to the three different values of r_0 . In particular, for some fixed temperature (e.g., $T = 0.16$) the algebraically lowest r_0 corresponds to the algebraically lowest Euclidean action; similarly, the medium and largest r_0 parameters correspond to the medium and largest Euclidean actions. The medium Euclidean action for the hairy black hole is very close to the Euclidean action for the topological black hole. In fact, it is slightly smaller than the latter for $T < \frac{1}{2\pi} \approx 0.159$ and slightly larger after that value. If it were the only branch present, one would thus conclude that the hairy black hole dominates for small temperatures, while for large temperatures

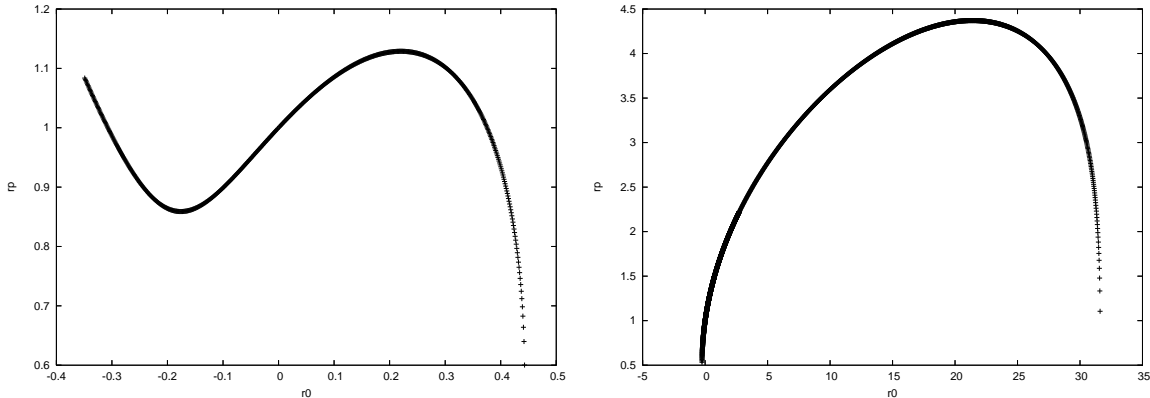


Figure 1: Horizon versus parameter r_0 for $g = 3$ (left panel) and $g = 0.0005$ (right panel).

the topological black hole would be preferred. This would be a situation similar to the one of the MTZ black hole.

However, the two additional branches change completely our conclusions. The upper branch shows that the hairy black hole dominates up to $T \approx 0.20$. When the coupling constant g decreases, equation (3.21) along with the demand that the temperature should be positive, show that the acceptable values of r_0 are two rather than three, as may be seen in figure 3, left panel. The lowest branch of the previous corresponding figure 2 shrinks for decreasing g and it finally disappears. An interesting consequence of this is that the temperature has an upper limit. The graph for the Euclidean actions (figure 3, right panel) is influenced accordingly. There are just two branches for the hairy black hole, rather than three in figure 2 and the figure ends on its right hand side at $T \approx 1.25$. The continuous line represents the Euclidean action for the topological black hole with the same temperature. Similar remarks hold as in the previous case, e.g., the phase transition moves to $T \approx 0.80$. In addition, the largest value of r_0 corresponds to the upper branch of the hairy black hole.

To understand the nature of this phase transition it is instructive to draw a kind of phase diagram, so that we can spot which is the dominant solution for a given pair of g and T . We depict our result in figure 4. The hairy solution dominates below the curve which shows the critical temperature as a function of the coupling constant g . The most striking feature of the graph is that the critical temperature diverges as $g \rightarrow 0$. Thus, it does not converge to the MTZ value $\frac{1}{2\pi} \approx 0.159$ at $g = 0$. For even the slightest nonzero values of g the critical temperature gets extremely large values! This appears to put the conformal point (MTZ black hole) in a special status within the set of these hairy black holes. In other words, the restoration of conformal invariance is not a smooth process, and the MTZ black hole solution cannot be obtained in a continuous way as $g \rightarrow 0$. In fact, it seems that (even infinitesimally) away from the conformal point $g = 0$ black holes are mostly hairy!

4 Stability Analysis

To perform the stability analysis of the hairy black hole it is more convenient to work in the Einstein frame. Henceforth, we shall work in units in which the radius of the boundary

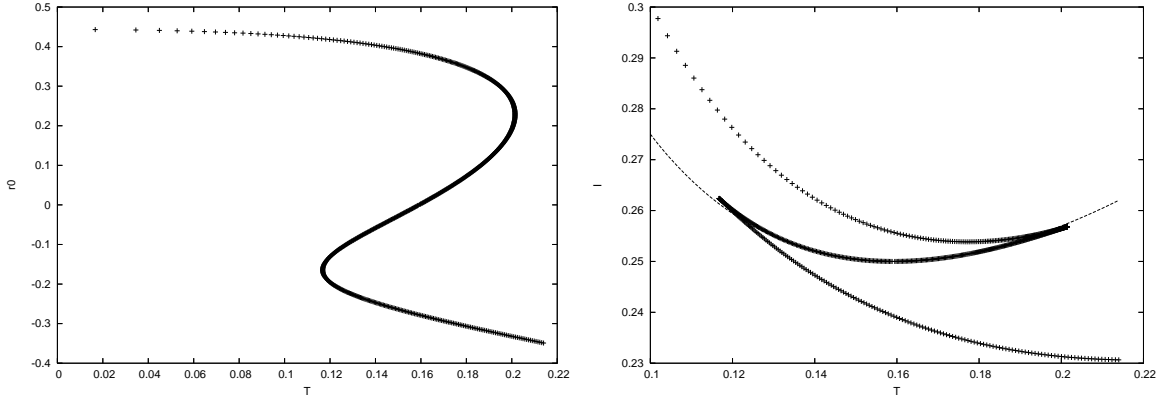


Figure 2: Parameter r_0 (left panel) and Euclidean actions versus temperature for $g = 3$ (right panel).

is $l = 1$.

We begin with the hairy black hole line element,

$$ds_0^2 = \frac{\hat{r}(\hat{r} + 2r_0)}{(\hat{r} + r_0)^2} \left[-F(\hat{r})dt^2 + \frac{d\hat{r}^2}{F(\hat{r})} + \hat{r}^2 d\sigma^2 \right], \quad (4.1)$$

which can be written in the form

$$ds^2 = -\frac{f_0}{h_0^2} dt^2 + \frac{dr^2}{f_0} + r^2 d\sigma^2 \quad (4.2)$$

using the definitions

$$\begin{aligned} f_0(r) &= F(\hat{r}) \left(1 + \frac{r_0^2}{(\hat{r} + 2r_0)(\hat{r} + r_0)} \right)^2, \\ h_0(r) &= \left(1 + \frac{r_0^2}{(\hat{r} + 2r_0)(\hat{r} + r_0)} \right) \frac{\hat{r} + r_0}{\sqrt{\hat{r}(\hat{r} + 2r_0)}}, \end{aligned} \quad (4.3)$$

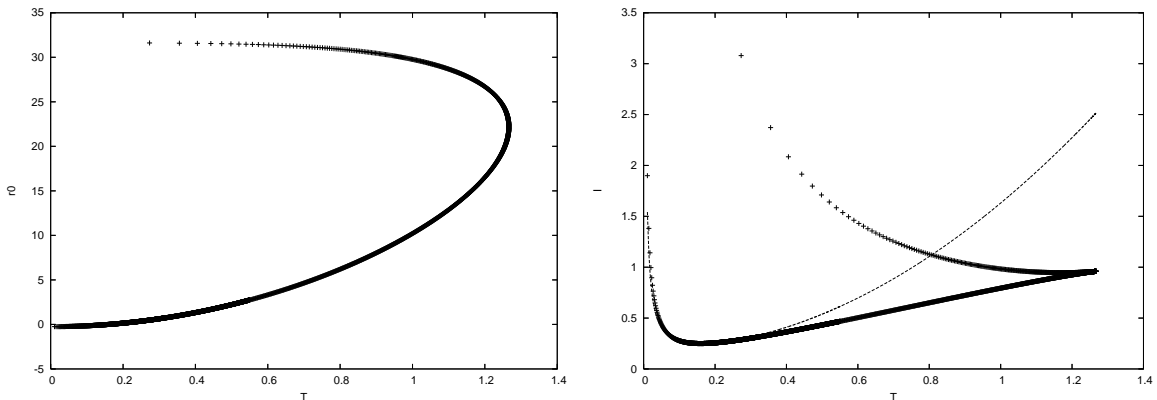


Figure 3: Parameter r_0 (left panel) and Euclidean actions versus temperature for $g = 0.0005$ (right panel).

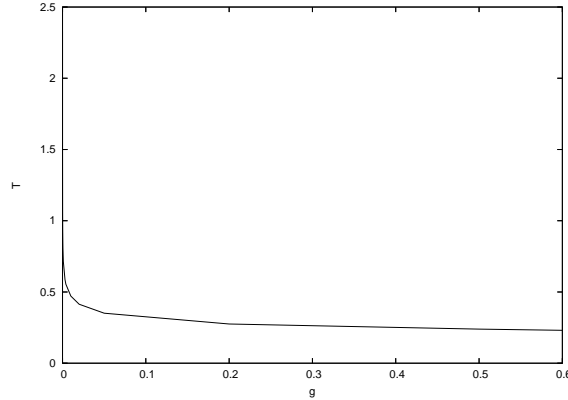


Figure 4: Phase diagram. For points under the curve the hairy solution will be preferred.

under the change of coordinates

$$r = \frac{\hat{r}^{3/2}(\hat{r} + 2r_0)^{1/2}}{\hat{r} + r_0} . \quad (4.4)$$

The scalar field solution reads

$$\phi_0(r) = \sqrt{\frac{3}{4\pi G}} \tanh^{-1} \frac{r_0}{\hat{r} + r_0} , \quad (4.5)$$

obeying the boundary conditions (2.8) with

$$\alpha = \alpha_0 = \sqrt{\frac{3}{4\pi G}} |r_0| . \quad (4.6)$$

We are interested in figuring out when the black hole is unstable (losing its hair to turn into a TBH) and discuss the results in the context of thermodynamic considerations. To this end, we apply the perturbation

$$f(r, t) = f_0(r) + f_1(r)e^{\omega t}, \quad h(r, t) = h_0(r) + h_1(r)e^{\omega t}, \quad \phi(r, t) = \phi_0(r) + \frac{\phi_1(r)}{r}e^{\omega t} . \quad (4.7)$$

which respects the boundary conditions (2.8) with $\omega > 0$ for an instability to develop.

The field equations read:

$$-1 - f - rf' + rf \frac{h'}{h} + 8\pi Gr^2 V(\phi) = 0 , \quad (4.8)$$

$$\dot{f} + rf\dot{\phi}\phi' = 0 , \quad (4.9)$$

$$2h' + rh \left[\frac{h^2}{f^2} \dot{\phi}^2 + \phi'^2 \right] = 0 , \quad (4.10)$$

$$\left(\frac{\dot{h}}{f} \dot{\phi} \right) - \frac{1}{r^2} \left(r^2 \frac{f}{h} \phi' \right)' + \frac{1}{h} V'(\phi) = 0 . \quad (4.11)$$

The field equations give a Schrödinger-like wave equation for the scalar perturbation,

$$-\frac{d^2\phi_1}{dr_*^2} + \mathcal{V}\phi_1 = -\omega^2\phi_1, \quad (4.12)$$

where we defined the tortoise coordinate

$$\frac{dr_*}{dr} = \frac{h_0}{f_0}, \quad (4.13)$$

and the effective potential is given by

$$\mathcal{V} = \frac{f_0}{h_0^2} \left[-\frac{1}{2}(1 + r^2\phi_0'^2)\phi_0'^2 f_0 + (1 - r^2\phi_0'^2)\frac{f_0'}{r} + 2r\phi_0'V'(\phi_0) + V''(\phi_0) \right]. \quad (4.14)$$

The explicit form of the Schrödinger-like equation reads:

$$-F(\hat{r})\frac{d}{d\hat{r}} \left[F(\hat{r})\frac{d\phi_1}{d\hat{r}} \right] + \mathcal{V}\phi_1 = -\omega^2\phi_1, \quad (4.15)$$

where the functional form of the function F has been given in equation (2.15) and ¹

$$\mathcal{V} = \frac{r_0^2 F(\hat{r})}{\hat{r}^2 \left(1 + \frac{2r_0}{\hat{r}}\right)^2 \left(1 + \frac{3r_0}{\hat{r}} + \frac{3r_0^2}{\hat{r}^2}\right)^2} \left\{ 5 + \frac{2 + (11g + 54)r_0^2}{r_0\hat{r}} + \frac{29 + (47g + 189)r_0^2}{\hat{r}^2} \right. \quad (4.16)$$

$$\left. + \frac{r_0(150 + (-3g + 270)r_0^2)}{\hat{r}^3} + \frac{r_0^2(396 + (-351g + 135)r_0^2)}{\hat{r}^4} + \frac{r_0^3(612 - 873gr_0^2)}{\hat{r}^5} \right. \quad (4.17)$$

$$\left. + \frac{r_0^4(582 - 1047gr_0^2)}{\hat{r}^6} + \frac{324r_0^5(1 - 2gr_0^2)}{\hat{r}^7} + \frac{81r_0^6(1 - 2gr_0^2)}{\hat{r}^8} \right. \quad (4.18)$$

$$\left. + \frac{g}{2} \left(5 + \frac{54r_0}{\hat{r}} + \frac{189r_0^2}{\hat{r}^2} + \frac{270r_0^3}{\hat{r}^3} + \frac{135r_0^4}{\hat{r}^4} \right) \ln \left(1 + \frac{2r_0}{\hat{r}} \right) \right\}. \quad (4.19)$$

Near the horizon the Schrödinger-like equation simplifies to

$$-[f'(\hat{r}_+)]^2 \epsilon \frac{d}{d\epsilon} \left[\epsilon \frac{d\phi_1}{d\epsilon} \right] = -\omega^2\phi_1, \quad \epsilon = \hat{r} - \hat{r}_+ \quad (4.20)$$

and its acceptable solution reads

$$\phi_1 \sim \epsilon^{\kappa\omega}, \quad \kappa = \frac{1}{f'(\hat{r}_+)}, \quad \omega > 0. \quad (4.21)$$

Regularity of the scalar field at the horizon ($r \rightarrow r_+$) requires the boundary conditions

$$\phi_1 = 0, \quad (r - r_+)\phi_1' = \kappa\omega\phi_1, \quad \kappa > 0. \quad (4.22)$$

¹We have set $8\pi G = 1$.

For a given $\omega > 0$, they uniquely determine the wavefunction.

At the boundary ($\hat{r} \rightarrow \infty$), the wave equation is approximated by

$$-\frac{d^2\phi_1}{dr_*^2} + 5r_0^2\phi_1 = -\omega^2\phi_1, \quad (4.23)$$

with solutions

$$\phi_1 = e^{\pm Er_*}, \quad E = \sqrt{\omega^2 + 5r_0^2}, \quad (4.24)$$

where $r_* = \int \frac{d\hat{r}}{f(\hat{r})} = -\frac{1}{r} + \dots$. Therefore, for large r ,

$$\phi_1 = A + \frac{B}{r} + \dots \quad (4.25)$$

To match the boundary conditions (2.8), we need

$$\frac{B}{A} = 2c\alpha_0 = -2r_0. \quad (4.26)$$

Since the wavefunction has already been determined by the boundary conditions at the horizon and therefore also the ratio B/A , this is a constraint on ω . If (4.26) has a solution, then the black hole is unstable. If it does not, then there is no instability of this type (however, one should be careful with non-perturbative instabilities).

In figure 5 (left panel) we show the ratio B/A for the standard MTZ black hole (corresponding to $g = 0$) versus ω at a typical value of the mass parameter, namely $r_0 = -0.10$. It is obvious that the value of the ratio lies well below the values $2r_0 = +0.20$. It is clearly impossible to have a solution to this equation, so the solution is stable. In fact this value of the mass parameter lies in the interesting range for this black hole, since thermodynamics dictates that for negative values of r_0 MTZ black holes are favored against topological black holes. We find that the MTZ black holes turn out to be stable.

Next we examine the case $g = 0.0005$, for which we have presented data before in figure 3. As we have explained there, the most interesting branch of the graphs is the upper branch, on the right panel, which dominates the small T part of the graph and corresponds to large values of r_0 (typically around 30 on the left panel of the same figure). Thus we set $g = 0.0005$, $r_0 = +30$ and plot B/A versus ω in the right panel of figure 5. It is clear that the curve lies systematically below the quantity $-2r_0 = -60$ and no solution is possible, so the hairy black hole with these parameters is stable.

Finally we come to the case with $g = +3$, which has three branches. In the left panel of figure 6 we show the results for $r_0 = +0.40$, which corresponds to the upper branch of figure 2; the curve again lies below the quantity $-2r_0 = -0.80$ and no solution is possible, so this hairy black hole is stable. In the right panel of figure 6 we show the results for $r_0 = -0.30$, which corresponds to the lowest branch of figure 2, which disappears for decreasing g . In this case we find something qualitatively different: the curve cuts the line $-2r_0 = +0.60$ around $\omega \approx 0.40$ and a solution is possible, signaling instability. Thus, for $g = 3$ the hairy black hole may be stable or unstable, depending on the value of r_0 .

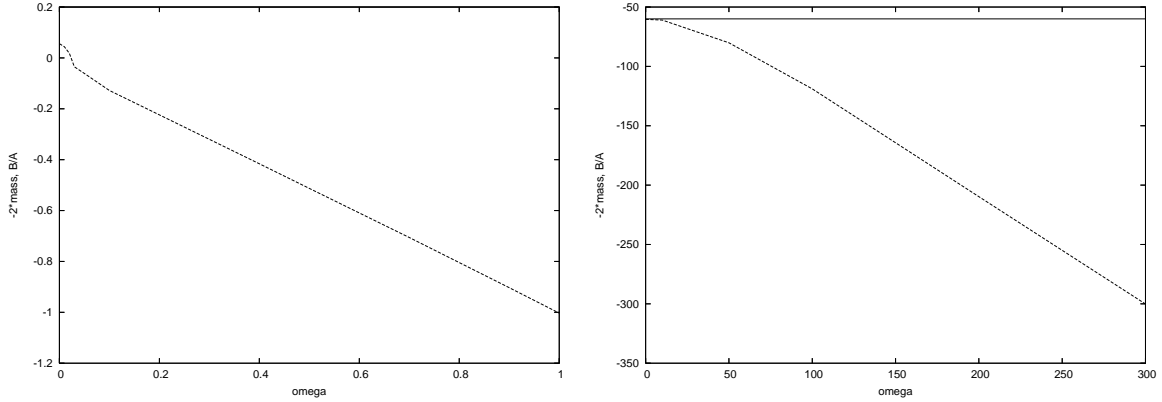


Figure 5: Stability of the standard MTZ black hole (left panel) for $r_0 = -0.10$; similarly for the hairy black hole at $g = 0.0005$, $r_0 = +30$ (right panel).

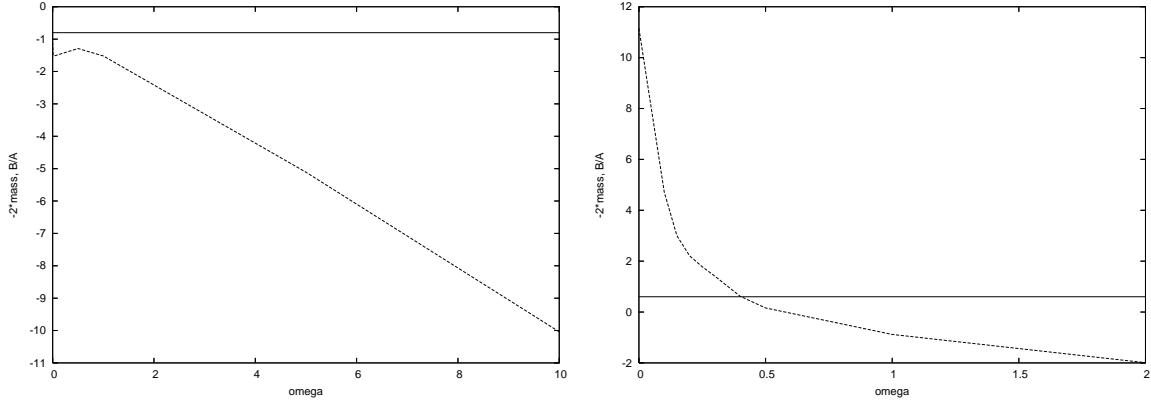


Figure 6: Stability of the hairy black hole for $g = 3$ and $r_0 = +0.40$ (left panel); similarly for the hairy black hole at $r_0 = -0.30$ (right panel).

5 Conclusions

We presented a new class of hairy black hole solutions in asymptotically AdS space. The scalar field is minimally coupled to gravity with a non-trivial self-interaction potential. A coupling constant g in the potential parametrizes our solutions. If $g = 0$ the conformal invariant MTZ black hole solution, conformally coupled to a scalar field, is obtained. If $g \neq 0$ a whole new class of hairy black hole solutions is generated. The scalar field is conformally coupled but the solutions are not conformally invariant. These solutions are perturbative stable near the conformal point for negative mass and they may develop instabilities for positive mass.

We studied the thermodynamical properties of the solutions. Calculating the free energy we showed that for a general g , apart the phase transition of the MTZ black hole at the critical temperature $T = 1/2\pi l$, there is another critical temperature, higher than the MTZ critical temperature, which depends on g and where a first order phase transition occurs of the vacuum black hole towards a hairy one. The existence of a second critical temperature is a manifestation of the breaking of conformal invariance. As $g \rightarrow 0$ the second critical

temperature diverges, indicating that there is no smooth limit to the MTZ solution.

The solutions presented and discussed in this work have hyperbolic horizons. There are also hairy black hole solutions with flat or spherical horizons of similar form. However, these solutions are pathological. In the solutions with flat horizons, the scalar field diverges at the horizon, in accordance to the “no-hair” theorems. In the case of spherical horizons, calculating the free energy we find that always the vacuum solution is preferable over the hairy configuration. Moreover, studying the asymptotic behaviour of the solutions, we found that they are unstable for any value of the mass.

Acknowledgments

G. S. was supported in part by the US Department of Energy under grant DE-FG05-91ER40627.

References

- [1] J. E. Chase, “Event horizons in static scalar-vacuum space-times,” *Commun. Math. Phys.* **19**, 276 (1970);
 J. D. Bekenstein, “Transcendence of the Law of Baryon-Number Conservation in Black-Hole Physics,” *Phys. Rev. Lett.* **28**, 452 (1972);
 J. D. Bekenstein, “Nonexistence of Baryon Number for Static Black Holes,” *Phys. Rev. D* **5**, 1239 (1972);
 J. D. Bekenstein, “Nonexistence of Baryon Number for Black Holes. II,” *Phys. Rev. D* **5**, 2403 (1972);
 M. Heusler, “A Mass Bound for Spherically Symmetric Black Hole Spacetimes,” *Class. Quant. Grav.* **12**, 779 (1995) [arXiv:gr-qc/9411054];
 M. Heusler and N. Straumann, “Scaling arguments for the existence of static, spherically symmetric solutions of self-gravitating systems,” *Class. Quant. Grav.* **9**, 2177 (1992);
 D. Sudarsky, “A simple proof of a no-hair theorem in Einstein-Higgs theory,” *Class. Quant. Grav.* **12**, 579 (1995);
 J. D. Bekenstein, “Novel ‘no-scalar-hair’ theorem for black holes,” *Phys. Rev. D* **51**, R6608 (1995).
- [2] A. E. Mayo and J. D. Bekenstein, “No hair for spherical black holes: charged and nonminimally coupled scalar field with self-interaction,” *Phys. Rev. D* **54**, 5059 (1996) [arXiv:gr-qc/9602057];
 J. D. Bekenstein, “Black hole hair: Twenty-five years after,” arXiv:gr-qc/9605059.
- [3] N. Bocharova, K. Bronnikov and V. Melnikov, *Vestn. Mosk. Univ. Fiz. Astron.* **6**, 706 (1970);
 J. D. Bekenstein, *Annals Phys.* **82**, 535 (1974);
 J. D. Bekenstein, “Black Holes With Scalar Charge,” *Annals Phys.* **91**, 75 (1975).

- [4] K. A. Bronnikov and Y. N. Kireyev, “Instability of black holes with scalar charge,” *Phys. Lett. A* **67**, 95 (1978).
- [5] K. G. Zloshchastiev, “On co-existence of black holes and scalar field,” *Phys. Rev. Lett.* **94**, 121101 (2005) [arXiv:hep-th/0408163].
- [6] T. Torii, K. Maeda and M. Narita, “No-scalar hair conjecture in asymptotic de Sitter spacetime,” *Phys. Rev. D* **59**, 064027 (1999) [arXiv:gr-qc/9809036].
- [7] C. Martinez, R. Troncoso and J. Zanelli, “de Sitter black hole with a conformally coupled scalar field in four dimensions,” *Phys. Rev. D* **67**, 024008 (2003) [arXiv:hep-th/0205319].
- [8] T. J. T. Harper, P. A. Thomas, E. Winstanley and P. M. Young, “Instability of a four-dimensional de Sitter black hole with a conformally coupled scalar field,” *Phys. Rev. D* **70**, 064023 (2004) [arXiv:gr-qc/0312104].
- [9] G. Dotti, R. J. Gleiser and C. Martinez, “Static black hole solutions with a self interacting conformally coupled scalar field,” *Phys. Rev. D* **77**, 104035 (2008) [arXiv:0710.1735 [hep-th]].
- [10] T. Torii, K. Maeda and M. Narita, “Scalar hair on the black hole in asymptotically anti-de Sitter spacetime,” *Phys. Rev. D* **64**, 044007 (2001).
- [11] E. Winstanley, “On the existence of conformally coupled scalar field hair for black holes in (anti-)de Sitter space,” *Found. Phys.* **33**, 111 (2003) [arXiv:gr-qc/0205092].
- [12] C. Martinez, R. Troncoso and J. Zanelli, “Exact black hole solution with a minimally coupled scalar field,” *Phys. Rev. D* **70**, 084035 (2004) [arXiv:hep-th/0406111].
- [13] C. Martinez, J. P. Staforelli and R. Troncoso, “Topological black holes dressed with a conformally coupled scalar field and electric charge,” *Phys. Rev. D* **74**, 044028 (2006) [arXiv:hep-th/0512022];
C. Martinez and R. Troncoso, “Electrically charged black hole with scalar hair,” *Phys. Rev. D* **74**, 064007 (2006) [arXiv:hep-th/0606130].
- [14] G. Koutsoumbas, E. Papantonopoulos and G. Siopsis, “Exact Gravity Dual of a Gapless Superconductor,” *JHEP* **0907**, 026 (2009) [arXiv:0902.0733 [hep-th]].
- [15] G. Koutsoumbas, S. Musiri, E. Papantonopoulos and G. Siopsis, “Quasi-normal modes of electromagnetic perturbations of four-dimensional topological black holes with scalar hair,” *JHEP* **0610**, 006 (2006) [arXiv:hep-th/0606096];
G. Koutsoumbas, E. Papantonopoulos and G. Siopsis, “Phase Transitions in Charged Topological-AdS Black Holes,” *JHEP* **0805**, 107 (2008) [arXiv:0801.4921 [hep-th]];
G. Koutsoumbas, E. Papantonopoulos and G. Siopsis, “Discontinuities in Scalar Perturbations of Topological Black Holes,” *Class. Quant. Grav.* **26**, 105004 (2009) [arXiv:0806.1452 [hep-th]].

- [16] C. Charmousis, T. Kolyvaris and E. Papantonopoulos, “Charged C-metric with conformally coupled scalar field,” *Class. Quant. Grav.* **26**, 175012 (2009) [arXiv:0906.5568 [gr-qc]].
- [17] A. Anabalón and H. Maeda, “New Charged Black Holes with Conformal Scalar Hair,” arXiv:0907.0219 [hep-th].
- [18] K. Farakos, A. P. Kouretsis and P. Pasipoularides, “Anti de Sitter 5D black hole solutions with a self-interacting bulk scalar field: a potential reconstruction approach,” *Phys. Rev. D* **80**, 064020 (2009) [arXiv:0905.1345 [hep-th]].
- [19] N. Ohta and T. Torii, “Black Holes in the Dilatonic Einstein-Gauss-Bonnet Theory in Various Dimensions IV - Topological Black Holes with and without Cosmological Term,” arXiv:0908.3918 [hep-th].
- [20] K.-I. Maeda, “Towards the Einstein-Hilbert action via conformal transformation,” *Phys. Rev. D* **39** 3159 (1989).
- [21] V. Faraoni, E. Gunzig and P. Nardone, *Fund. Cosmic Phys.* **20**, 121 (1999) [arXiv:gr-qc/9811047].
- [22] V. Faraoni and S. Sonego, “On The Tail Problem In Cosmology,” *Phys. Lett. A* **170**, 413 (1992) [arXiv:astro-ph/9209004];
T. W. Noonan, “Huygen’s principle in conformally flat spacetimes,” *Class. Quant. Grav.* **12**, 1087 (1995).
- [23] T. Hertog and K. Maeda, “Stability and thermodynamics of AdS black holes with scalar hair,” *Phys. Rev. D* **71**, 024001 (2005) [arXiv:hep-th/0409314].
- [24] S. A. Hartnoll, C. P. Herzog and G. T. Horowitz, “Building a Holographic Superconductor,” *Phys. Rev. Lett.* **101**, 031601 (2008) [arXiv:0803.3295 [hep-th]].
- [25] S. A. Hartnoll, C. P. Herzog and G. T. Horowitz, “Holographic Superconductors,” *JHEP* **0812**, 015 (2008) [arXiv:0810.1563 [hep-th]].
- [26] D. F. Zeng, “An Exact Hairy Black Hole Solution for AdS/CFT Superconductors,” arXiv:0903.2620 [hep-th].
- [27] R. B. Mann, “Topological Black Holes – Outside Looking In,” arXiv:gr-qc/9709039.
- [28] D. Birmingham, “Topological Black Holes in Anti-de Sitter Space,” *Class. Quant. Grav.* **16**, 1197 (1999) [arXiv:hep-th/9808032].
- [29] A. Ashtekar and S. Das, “Asymptotically Anti-de Sitter Space-times: Conserved Quantities,” *Class. Quant. Grav.* **17**, L17 (2000) [arXiv:hep-th/9911230].